Open camera or QR reader and
scan code to access this article
and other resources online.

Epitope Mapping of an Anti-Mouse CD39 Monoclonal Antibody Using PA Scanning and RIEDL Scanning

Yuki Okada, Hiroyuki Suzuki, Tomohiro Tanaka, Mika K. Kaneko, and Yukinari Kato

A cell-surface ectonucleotidase CD39 mediates the conversion of extracellular adenosine triphosphate into immunosuppressive adenosine with another ectonucleotidase CD73. The elevated adenosine in the tumor microenvironment attenuates antitumor immunity, which promotes tumor cell immunologic escape and progression. Anti-CD39 monoclonal antibodies (mAbs), which suppress the enzymatic activity, can be applied to antitumor therapy. Therefore, an understanding of the relationship between the inhibitory activity and epitope of mAbs is important. We previously established an anti-mouse CD39 (anti-mCD39) mAb, C_{39}Mab-1 using the Cell-Based Immunization and Screening method. In this study, we determined the critical epitope of C_{39}Mab-1 using flow cytometry. We performed the PA tag (12 amino acids [aa])-substituted analysis (named PA scanning) and RIEDL tag (5 aa)-substituted analysis (named RIEDL scanning) to determine the critical epitope of C_{39}Mab-1 using flow cytometry. By the combination of PA scanning and RIEDL scanning, we identified the conformational epitope, spanning three segments of 275–279, 282–291, and 306–323 aa of mCD39. These analyses would contribute to the identification of the conformational epitope of membrane proteins.

Keywords: mouse CD39, monoclonal antibody, epitope, PA scanning, RIEDL scanning

Introduction

IN THE TUMOR MICROENVIRONMENT (TME), high concentrations of extracellular adenosine triphosphate (ATP) (100 to 500 μM) exist compared to nanomolar order in normal tissues due to the passive release of cell death and active secretion by tumor cells and other subsets.[1–3] The extracellular adenosine, produced by the hydrolysis of extracellular ATP, is involved in immunosuppressive TME[4] and suppresses antitumor immune responses and enhances the immunologic escape of tumor cells.[5] Therefore, the extent of ATP release and its degradation to adenosine should be controlled to restrict the immunosuppressive TME and to facilitate the antitumor immunity during cancer immunotherapy.[6,7]

CD39 (ectonucleoside triphosphate diphosphohydrolase 1; encoded by *ENTPD1*) protein has 510 amino acids (aa) and harbors 7 potential *N*-linked glycosylation sites and 11 cysteine residues.[8] Two transmembrane domains exist in the CD39 protein. In the extracellular domain of CD39, five highly conserved segments mediate the enzymatic activity to

catalyze the hydrolysis of extracellular ATP and adenosine diphosphate to adenosine monophosphate. Then, CD73 (5′-nucleotidase; encoded by NT5E) dephosphorylates AMP into adenosine.[9]

Since CD39 mediates the dephosphorylation of extracellular ATP to immunosuppressive adenosine, anti-CD39 monoclonal antibodies (mAbs) have been generated to modulate the adenosine metabolism.[6] A preclinical study showed that B66, an anti-mouse CD39 (mCD39) mAb, can inhibit mCD39 enzymatic activity *in vitro* and exerted the antitumor effect by the mono- or combination therapy with the PD-1 blockade.[10] The anti-human CD39 mAbs, such as TTX-030, IPH5201, and SRF-617, were designed to inhibit the CD39 enzymatic activity.[7,10] These mAbs have been evaluated in clinical trials for solid tumors in combination with chemotherapeutic agents or immune checkpoint inhibitors.[8] However, the relationship between the inhibitory activity and the epitope has not been clarified.

We previously established a novel anti-mCD39 mAb (C_{39}Mab-1) by the Cell-Based Immunization and Screening

---

Department of Antibody Drug Development, Tohoku University Graduate School of Medicine, Sendai, Miyagi, Japan.

(CBIS) method,[11–36] and evaluated its applications, including flow cytometry and western blot analyses.[37] In this study, we performed epitope mapping of C_{39}Mab-1 using flow cytometry-mediated novel strategies, named PA scanning and RIEDL scanning.

Materials and Methods

Antibodies

C_{39}Mab-1 (an anti-mCD39 mAb),[37] LpMab-7 (an anti-RIEDL [R*] tag mAb),[38–46] and NZ-1 (an anti-PA tag mAb)[47–53] were described previously. An anti-mCD39 mAb (clone 5F2, mouse IgG$_1$, kappa) was purchased from BioLegend (San Diego, CA). Alexa Fluor 488-conjugated anti-mouse IgG and anti-rat IgG were purchased from Cell Signaling Technology, Inc. (Danvers, MA).

Plasmid construction and transfection

mCD39 cDNA was cloned into a pCAG-Ble vector (FUJIFILM Wako Pure Chemical Corporation, Osaka, Japan). For PA scanning, the substitution of PA tag (GVAMPGAEDDVV) in mCD39 was performed with oligonucleotides containing PA tag sequence at the desired position. For example, for the substitution of the PA tag from K288 to P299 of mCD39, we constructed E287-GVAMPGAEDDVV-C300 ($_{288}$-PA-$_{299}$) in mCD39. For RIEDL scanning, the substitution of the R* tag in mCD39 was performed with oligonucleotides containing the R* tag sequence at the desired position. For example, for the substitution of the R* tag from E287 to N291 of mCD39, we constructed Y286-RIEDL-V292 ($_{287}$-R*-$_{291}$) in mCD39.

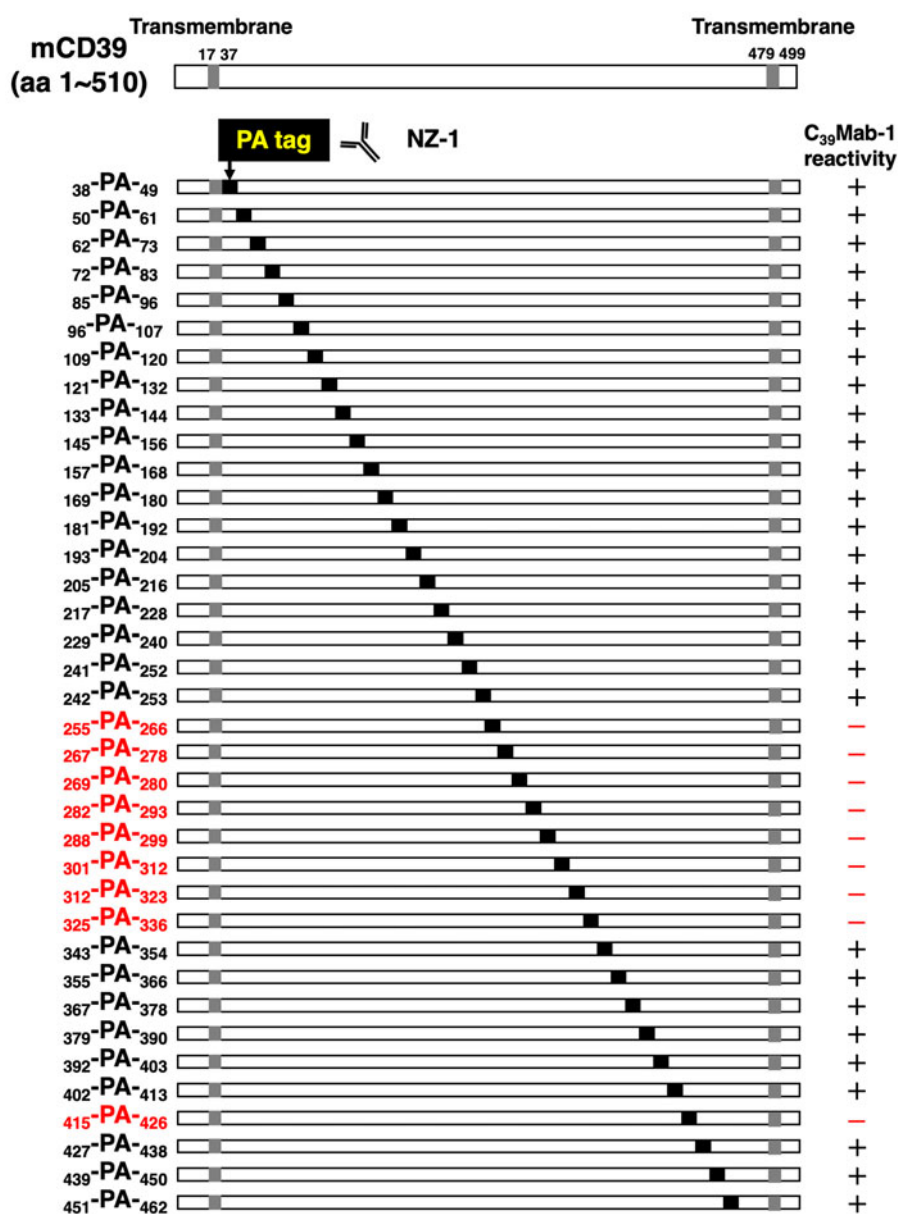Alanine scanning in the mCD39 sequence was performed with oligonucleotides containing the alanine sequence at the

FIG. 1. The PA tag-substituted mutants of mCD39. The reactivities of C_{39}Mab-1 are indicated: +, reactive; −, nonreactive. mCD39, mouse CD39.
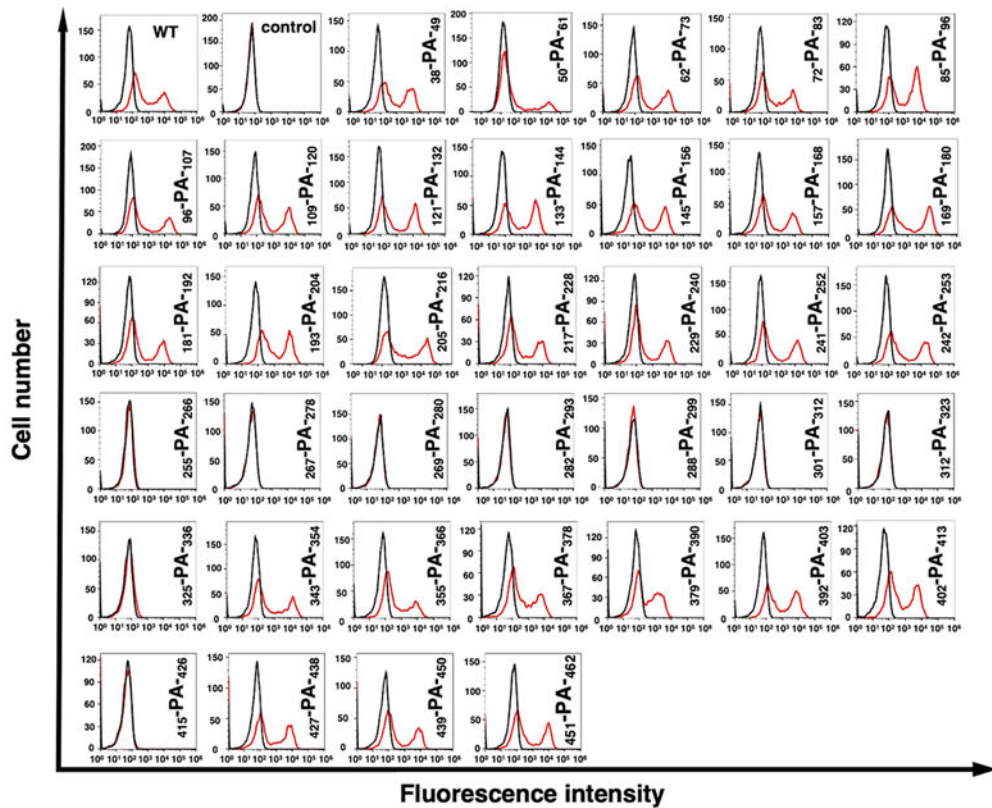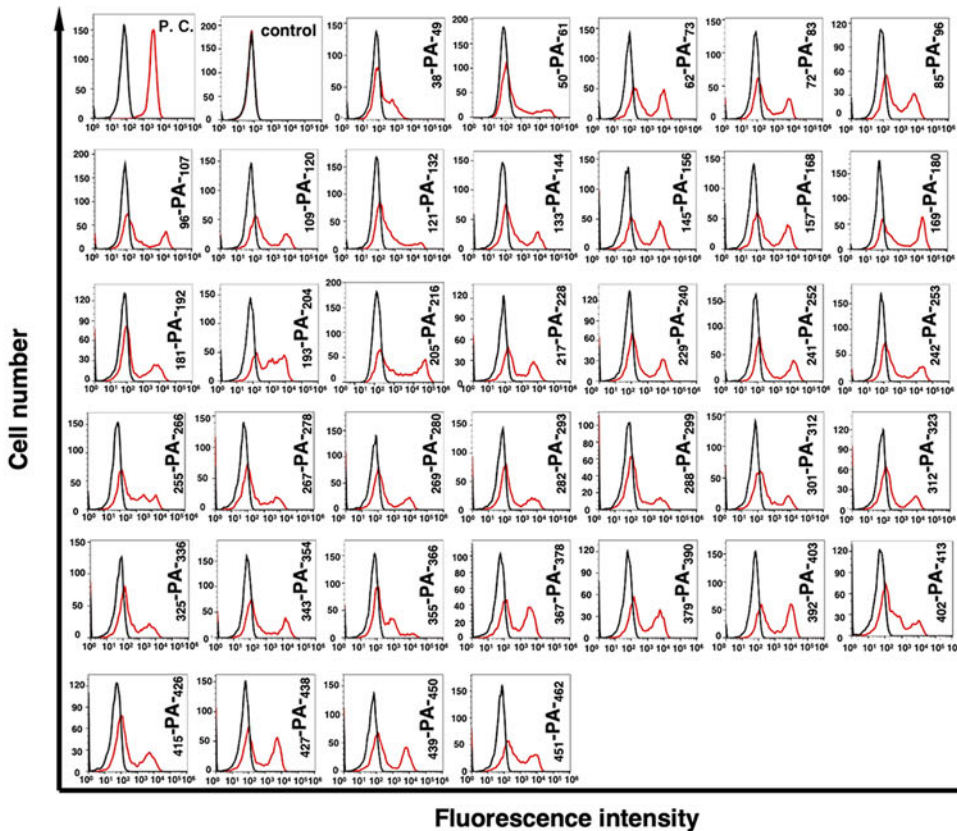
FIG. 2. Epitope determination of C_{39}Mab-1 using PA tag-substituted mutants of mCD39. The PA tag-substituted mutants of mCD39 were transiently expressed in CHO-K1 cells. The mutants-expressed CHO-K1 cells were incubated with 1 μg/mL of C_{39}Mab-1 (**A**, red line), 1 μg/mL of NZ-1 (**B**, red line), or control blocking buffer (black line), followed by secondary antibodies treatment. The data were analyzed using the SA3800 Cell Analyzer. CHO, Chinese hamster ovary; P. C., positive control (CHO/PA-CD133); WT, wild type mCD39.

desired position. The PCR fragments bearing the desired mutations were inserted into the pCAG-Ble vector (FUJI-FILM Wako Pure Chemical Corporation) using an In-Fusion HD Cloning Kit (Takara Bio, Inc., Shiga, Japan).

The mCD39 mutant plasmids were transiently transfected into Chinese hamster ovary (CHO)-K1 cells (the American Type Culture Collection, Manassas, VA) using the Neon Transfection System (Thermo Fisher Scientific, Inc., Waltham, MA). CHO-K1 cells and transfectants were cultured in Roswell Park Memorial Institute-1640 medium (Nacalai Tesque, Inc., Kyoto, Japan) supplemented with 10% heat-inactivated fetal bovine serum (Thermo Fisher Scientific, Inc.), 100 units/mL of penicillin, 100 μg/mL of streptomycin, and 0.25 μg/mL of amphotericin B (Nacalai Tesque, Inc.). The cells were cultured at 37°C in a humidified atmosphere containing 5% carbon dioxide and 95% air.

Flow cytometry

CHO-K1 cells and transfectants were harvested after a brief exposure to 0.25% trypsin in 1 mM ethylenediamine-tetraacetic acid (Nacalai Tesque, Inc.) and washed with 0.1% bovine serum albumin in phosphate-buffered saline. C_{39}Mab-1 (1 μg/mL), LpMab-7 (10 μg/mL), or NZ-1 (1 μg/mL) were incubated for 30 minutes at 4°C. The cells were further treated with Alexa Fluor 488-conjugated anti-mouse IgG (1:2000 for LpMab-7 and 5F2) or anti-rat IgG (1:2000 for C_{39}Mab-1 and NZ-1). Fluorescence data were collected using the SA3800 Cell Analyzer (Sony Corp., Tokyo, Japan).

Results

Epitope mapping of C_{39}Mab-1 using flow cytometry with PA tag-substituted mCD39

We previously established an anti-mCD39 mAb (C_{39}Mab-1) by the CBIS method.[37] To determine the C_{39}Mab-1 epitope, we first examined the reactivity to the peptides that cover the extracellular domain of mCD39. However, C_{39}Mab-1 did not react with the peptides (data not shown), suggesting that C_{39}Mab-1 recognizes a conformational and/or modified epitope.

To identify the binding epitope of C_{39}Mab-1, we generated PA tag (GVAMPGAEDDVV)-substituted mCD39 mutants as shown in Figure 1. We analyzed the reactivity of C_{39}Mab-1 against the PA tag-substituted mCD39 (named PA scanning). As shown in Figure 2A, the reactivity of C_{39}Mab-1 almost completely disappeared in $_{255}$-PA-$_{266}$, $_{267}$-PA-$_{278}$, $_{269}$-PA-$_{280}$, $_{282}$-PA-$_{293}$, $_{288}$-PA-$_{299}$, $_{301}$-PA-$_{312}$, $_{312}$-PA-$_{323}$, $_{325}$-PA-$_{336}$, and $_{415}$-PA-$_{426}$ mutants of mCD39. In contrast, the reactivity of C_{39}Mab-1 was observed in the PA tag-substituted mutants of 38–253, 343–413, and 427–462 aa. The cell surface expression of each mutant was confirmed by an anti-PA tag mAb, NZ-1 (Fig. 2B). The reactivity was summarized in Figure 1. These results indicated that the epitope of C_{39}Mab-1 contains 255–336 and 415–426 aa of mCD39.

Epitope mapping of C_{39}Mab-1 using flow cytometry with RIEDL tag-substituted mCD39

As shown in Figure 2A, C_{39}Mab-1 did not react with the continuous PA tag-substituted region of 255–336 aa in
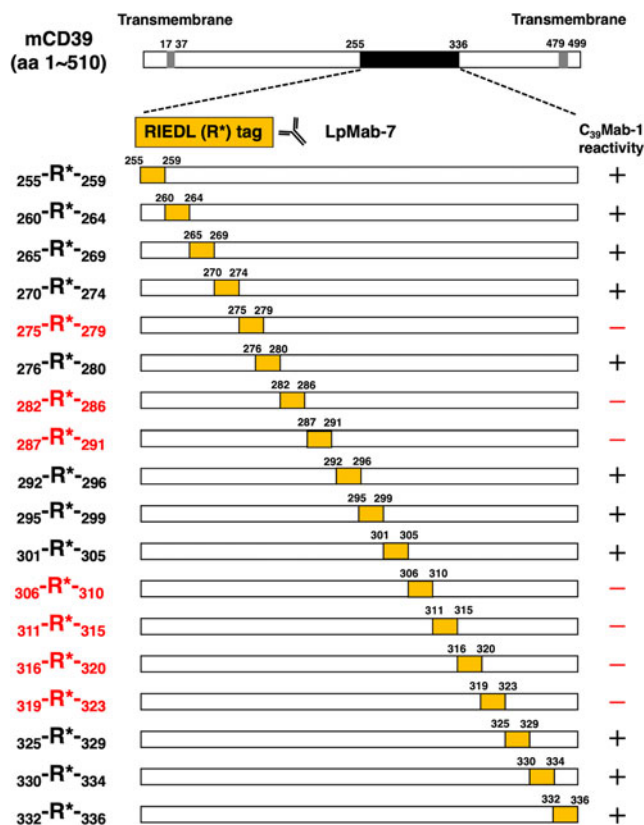

FIG. 3. The RIEDL tag-substituted mutants of mCD39. The reactivities of C_{39}Mab-1 are indicated: +, reactive; −, nonreactive.

mCD39. We generated the R* tag-substituted mCD39 as shown in Figure 3 to narrow down the C_{39}Mab-1 epitope. We analyzed the reactivity of C_{39}Mab-1 against the R* tag-substituted mCD39 (named RIEDL scanning). As shown in Figure 4A, the reactivity of C_{39}Mab-1 almost completely disappeared in $_{275}$-R*-$_{279}$, $_{282}$-R*-$_{286}$, $_{287}$-R*-$_{291}$, $_{306}$-R*-$_{310}$, $_{311}$-R*-$_{315}$, $_{316}$-R*-$_{320}$, and $_{319}$-R*-$_{323}$ mutants of mCD39. In contrast, the reactivity of C_{39}Mab-1 was observed in R* tag-substituted mutants of 255–274, 276–280, 292–305, and 325–336 aa. The cell surface expression of each mutant was confirmed by an anti-R* tag mAb, LpMab-7 (Fig. 4B). The reactivity was summarized in Figure 3. These results narrowed down the epitope of C_{39}Mab-1 in 275–279, 282–291, and 306–323 aa of mCD39.

Epitope mapping of C_{39}Mab-1 using flow cytometry with 1×alanine- or 2×alanine-substituted mCD39

The 1×alanine- or 2×alanine-substituted mutant analyses are important strategies to determine the center of the epitope.[54–56] We next generated 33 alanine-substituted mCD39 in 275th to 323rd aa of mCD39 and investigated the reactivity of C_{39}Mab-1 against CHO-K1 cells, which overexpressed the mCD39 mutants transiently. As a result, C_{39}Mab-1 reacted with all alanine-substituted mutants and wild type (Supplementary Fig. S1).

We also examined the reactivity of C_{39}Mab-1 against 2×alanine-substituted mCD39; however, C_{39}Mab-1 reacted
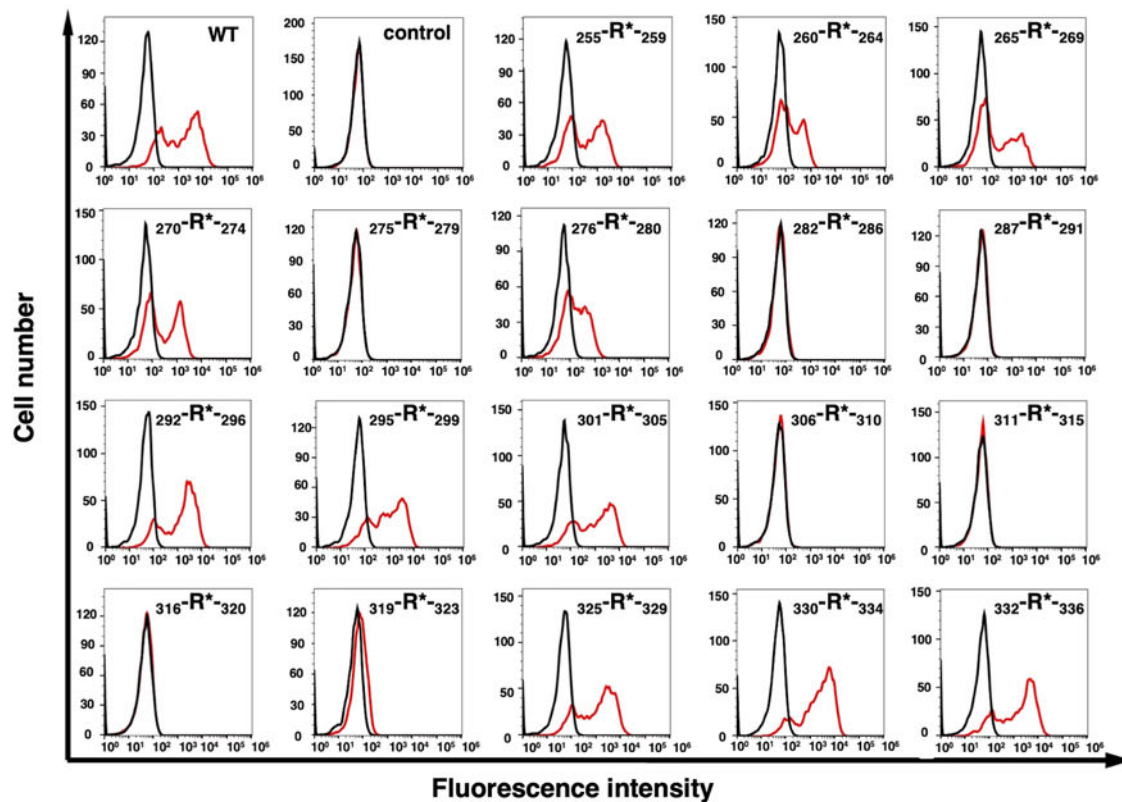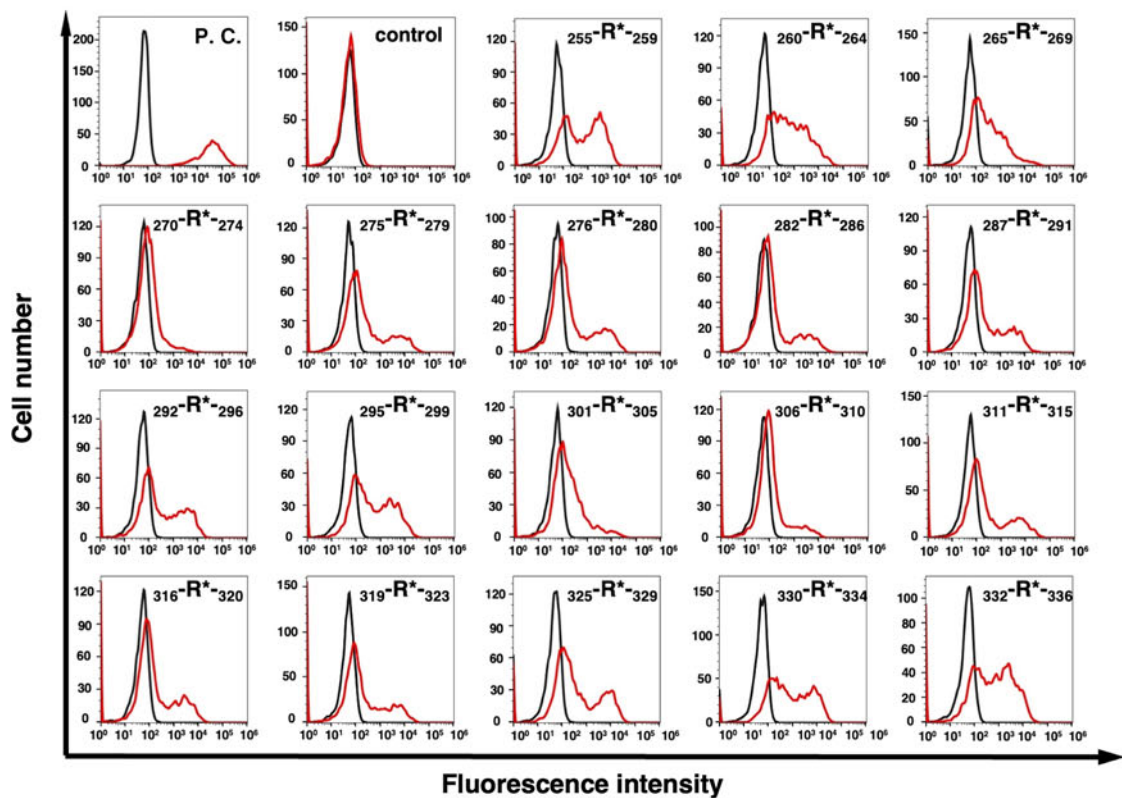
FIG. 4. Epitope determination of C_{39}Mab-1 using RIEDL tag-substituted mutants of mCD39. The RIEDL (R*) tag-substituted mutants of mCD39 were transiently expressed in CHO-K1 cells. The mutants-expressed CHO-K1 cells were incubated with 1 µg/mL of C_{39}Mab-1 (**A**, red line), 10 µg/mL of LpMab-7 (**B**, red line), or control blocking buffer (black line), followed by secondary antibodies treatment. The data were analyzed using the SA3800 Cell Analyzer. P. C., positive control (CHO/2×RIEDL-seaPDPN).[24]
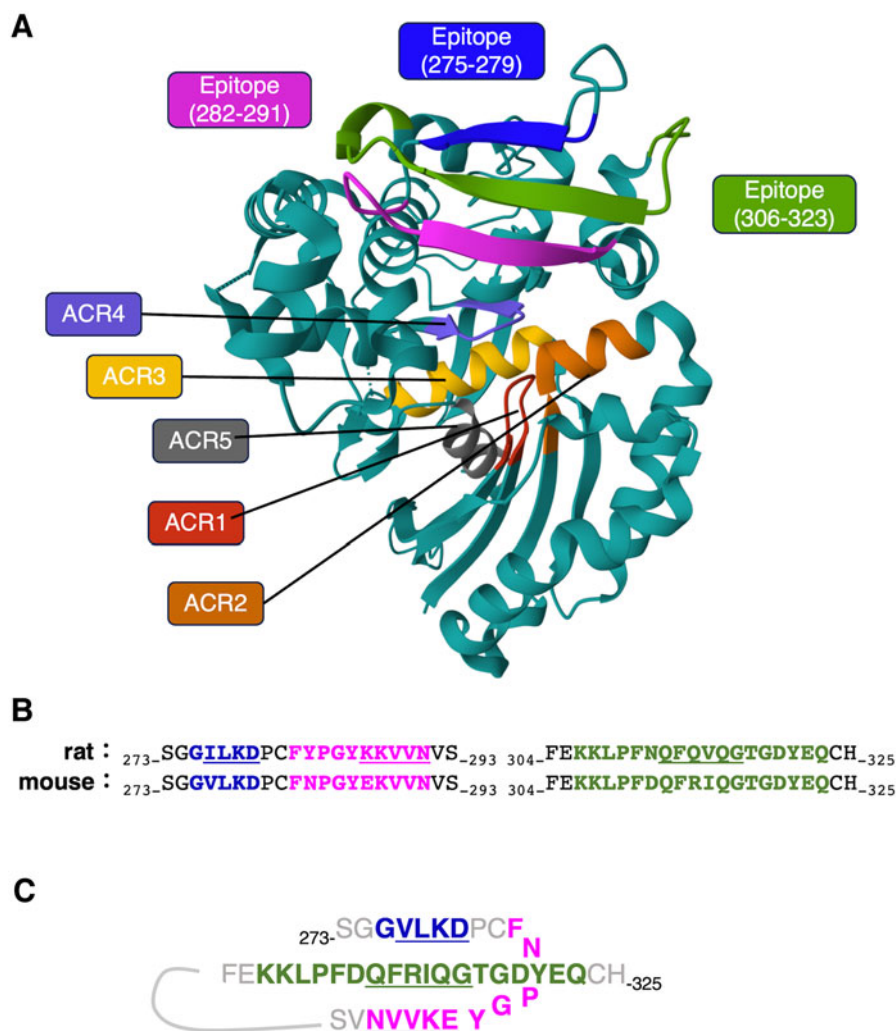
48

FIG. 5. Structure of CD39 and putative epitope of C$_{39}$Mab-1. **(A)** Rat CD39 structure (PDB ID: 3ZX3). The corresponding sequence to the three segments of C$_{39}$Mab-1 epitope segments is highlighted. Apyrase-conserved regions (ACR1–5) are also indicated. **(B)** The alignment of rat and mouse CD39 sequence around C$_{39}$Mab-1 epitope segments. The underlined sequences form a β-sheet as shown in **(A)**. **(C)** Putative β-sheet structure of C$_{39}$Mab-1 epitope segments.

with all mutants (Supplementary Fig. S2). Therefore, we could not determine the epitope of C$_{39}$Mab-1 using 1×alanine or 2×alanine scanning methods.

Discussion

In this study, we performed the flow cytometry-based epitope mapping of C$_{39}$Mab-1 using the PA scanning (Figs. 1, 2) and the RIEDL scanning (Figs. 3, 4). We found that the three segments, 275–279, 282–291, and 306–323 aa of mCD39 are important for the recognition by C$_{39}$Mab-1.

Zebisch *et al.* demonstrated the crystal structure of rat CD39 between the two lobes of the catalytic domain.[57] Figure 5A shows the structure of rat CD39 (PDB ID: 3ZX3). Apyrase-conserved regions (ACR1–5) form the active-site cleft,[58] which is distant from the three segments identified as C$_{39}$Mab-1 epitope. As shown in Figure 5B, the corresponding rat CD39 sequence to the three segments forms a β-sheet structure. In mouse sequence motifs, $_{276}$-VLKD-$_{279}$, $_{287}$-EKVVN-$_{291}$, and $_{312}$-QFRIQG-$_{317}$ could contribute to

the formation of the β-sheet (Fig. 5C). The substitution of the R* tag on not only the above three motifs but also surrounding sequence may disrupt the β-sheet structure, which results in the impaired recognition by C$_{39}$Mab-1. Although we could not determine the critical aa of the epitope by 1×alanine or 2×alanine scanning methods (Supplementary Figs. S1, S2), it would be interesting to introduce mutations between some β-sheet segments and examine the reactivity of C$_{39}$Mab-1.

Therapeutic anti-CD39 mAbs, including TTX-030, were designed to inhibit CD39 enzymatic activity through the uncompetitive allosteric mechanism of action.[7,10] The epitope of TTX-030 was determined as E142 to Y159 using the human-mouse CD39 chimeric protein by flow cytometry.[59] The region is distal to the ATP-binding residues (E174 and S218), supporting the allosteric mechanism of action by TTX-030. However, the optimal mAb-binding sites to inhibit the CD39 enzymatic activity have not been identified. Therefore, the detailed relationship between each mAb epitope and the inhibitory activity should be determined. The PA

scanning and RIEDL scanning would contribute to the determination of the conformational epitope of not only CD39 but also other membranous antigens.

Acknowledgment

Authors' Contributions

Y.O. and T.T. performed the experiments. M.K.K. and Y.K. designed the experiments. H.S. and M.K.K. analyzed the data. H.S. and Y.K. wrote the article. All authors have read and agreed to the published version of the article.

Author Disclosure Statement

No competing financial interests exist.

Funding Information

Supplementary Material

Supplementary Figure S1
Supplementary Figure S2

References

1. Di Virgilio F, Adinolfi E. Extracellular purines, purinergic receptors and tumor growth. Oncogene 2017;36:293–303; doi: 10.1038/onc.2016.206

2. Grygorczyk R, Boudreault F, Ponomarchuk O, et al. Lytic release of cellular ATP: Physiological relevance and therapeutic applications. Life (Basel) 2021;11; doi: 10.3390/life11070700

3. Di Virgilio F, Sarti AC, Falzoni S, et al. Extracellular ATP and P2 purinergic signalling in the tumour microenvironment. Nat Rev Cancer 2018;18:601–618; doi: 10.1038/s41568-018-0037-0

4. Vijayan D, Young A, Teng MWL, et al. Targeting immunosuppressive adenosine in cancer. Nat Rev Cancer 2017;17:709–724; doi: 10.1038/nrc.2017.86

5. Guo S, Han F, Zhu W. CD39—a bright target for cancer immunotherapy. Biomed Pharmacother 2022;151:113066; doi: 10.1016/j.biopha.2022.113066

6. Xia C, Yin S, To KKW, et al. CD39/CD73/A2AR pathway and cancer immunotherapy. Mol Cancer 2023;22:44; doi: 10.1186/s12943-023-01733-x

7. Perrot I, Michaud HA, Giraudon-Paoli M, et al. Blocking antibodies targeting the CD39/CD73 immunosuppressive pathway unleash immune responses in combination cancer therapies. Cell Rep 2019;27:2411–2425.e2419; doi: 10.1016/j.celrep.2019.04.091

8. Moesta AK, Li XY, Smyth MJ. Targeting CD39 in cancer. Nat Rev Immunol 2020;20:739–755; doi: 10.1038/s41577-020-0376-4

9. Liu Y, Li Z, Zhao X, et al. Review immune response of targeting CD39 in cancer. Biomark Res 2023;11:63; doi: 10.1186/s40364-023-00500-w

10. Li XY, Moesta AK, Xiao C, et al. Targeting CD39 in cancer reveals an extracellular ATP- and inflammasome-driven tumor immunity. Cancer Discov 2019;9:1754–1773; doi: 10.1158/2159-8290.Cd-19-0541

11. Tawara M, Suzuki H, Goto N, et al. A novel anti-CD44 variant 9 monoclonal antibody C(44)Mab-1 was developed for immunohistochemical analyses against colorectal cancers. Curr Issues Mol Biol 2023;45:3658–3673; doi: 10.3390/cimb45040238

12. Suzuki H, Kitamura K, Goto N, et al. A novel anti-CD44 variant 3 monoclonal antibody C(44)Mab-6 was established for multiple applications. Int J Mol Sci 2023;24; doi: 10.3390/ijms24098411

13. Suzuki H, Goto N, Tanaka T, et al. Development of a novel anti-CD44 variant 8 monoclonal antibody C(44)Mab-94 against gastric carcinomas. Antibodies (Basel) 2023;12; doi: 10.3390/antib12030045

14. Kudo Y, Suzuki H, Tanaka T, et al. Development of a novel anti-CD44 variant 5 monoclonal antibody C(44)Mab-3 for multiple applications against pancreatic carcinomas. Antibodies (Basel) 2023;12; doi: 10.3390/antib12020031

15. Ishikawa K, Suzuki H, Kaneko MK, et al. Establishment of a novel anti-CD44 variant 10 monoclonal antibody C(44)Mab-18 for immunohistochemical analysis against oral squamous cell carcinomas. Curr Issues Mol Biol 2023;45:5248–5262; doi: 10.3390/cimb45070333

16. Goto N, Suzuki H, Tanaka T, et al. EMab-300 detects mouse epidermal growth factor receptor-expressing cancer cell lines in flow cytometry. Antibodies (Basel) 2023;12; doi: 10.3390/antib12030042

17. Ejima R, Suzuki H, Tanaka T, et al. Development of a novel anti-CD44 variant 6 monoclonal antibody C(44)Mab-9 for multiple applications against colorectal carcinomas. Int J Mol Sci 2023;24; doi: 10.3390/ijms24044007

18. Nanamiya R, Suzuki H, Takei J, et al. Development of monoclonal antibody 281-mG(2a)-f against golden hamster podoplanin. Monoclon Antib Immunodiagn Immunother 2022;41:311–319; doi: 10.1089/mab.2021.0058

19. Li G, Suzuki H, Asano T, et al. Development of a novel anti-EpCAM monoclonal antibody for various applications. Antibodies (Basel) 2022;11; doi: 10.3390/antib11020041

20. Goto N, Suzuki H, Tanaka T, et al. Development of a monoclonal antibody PMab-292 against ferret podoplanin. Monoclon Antib Immunodiagn Immunother 2022;41:101–109; doi: 10.1089/mab.2021.0067

21. Asano T, Suzuki H, Tanaka T, et al. C(3)Mab-3: A monoclonal antibody for mouse CC chemokine receptor 3 for flow cytometry. Monoclon Antib Immunodiagn Immunother 2022;41:74–79; doi: 10.1089/mab.2021.0062

22. Tanaka T, Ohishi T, Asano T, et al. An anti-TROP2 monoclonal antibody TrMab-6 exerts antitumor activity in breast cancer mouse xenograft models. Oncol Rep 2021;46; doi: 10.3892/or.2021.8083

23. Tanaka T, Nanamiya R, Takei J, et al. Development of anti-mouse CC chemokine receptor 8 monoclonal antibodies for flow cytometry. Monoclon Antib Immunodiagn Immunother 2021;40:65–70; doi: 10.1089/mab.2021.0005

24. Tanaka T, Asano T, Sano M, et al. Development of monoclonal antibody PMab-269 against California sea lion podoplanin. Monoclon Antib Immunodiagn Immunother 2021;40:124–133; doi: 10.1089/mab.2021.0011

25. Takei J, Asano T, Nanamiya R, et al. Development of anti-human T cell immunoreceptor with Ig and ITIM domains (TIGIT) monoclonal antibodies for flow cytometry. Monoclon Antib Immunodiagn Immunother 2021;40:71–75; doi: 10.1089/mab.2021.0006

26. Sayama Y, Kaneko MK, Kato Y. Development and characterization of TrMab-6, a novel anti-TROP2 monoclonal antibody for antigen detection in breast cancer. Mol Med Rep 2021;23; doi: 10.3892/mmr.2020.11731

27. Nanamiya R, Takei J, Asano T, et al. Development of anti-human CC chemokine receptor 9 monoclonal antibodies for flow cytometry. Monoclon Antib Immunodiagn Immunother 2021;40:101–106; doi: 10.1089/mab.2021.0007

28. Hosono H, Asano T, Takei J, et al. Development of an anti-elephant podoplanin monoclonal antibody PMab-265 for flow cytometry. Monoclon Antib Immunodiagn Immunother 2021;40:141–145; doi: 10.1089/mab.2021.0015

29. Yamada S, Kaneko MK, Sayama Y, et al. Development of novel mouse monoclonal antibodies against human CD19. Monoclon Antib Immunodiagn Immunother 2020;39:45–50; doi: 10.1089/mab.2020.0003

30. Kaneko MK, Sano M, Takei J, et al. Development and characterization of anti-sheep podoplanin monoclonal antibodies PMab-253 and PMab-260. Monoclon Antib Immunodiagn Immunother 2020;39:144–155; doi: 10.1089/mab.2020.0018

31. Kaneko MK, Ohishi T, Kawada M, et al. A cancer-specific anti-podocalyxin monoclonal antibody (60-mG(2a)-f) exerts antitumor effects in mouse xenograft models of pancreatic carcinoma. Biochem Biophys Rep 2020;24:100826; doi: 10.1016/j.bbrep.2020.100826

32. Furusawa Y, Kaneko MK, Kato Y. Establishment of C(20)Mab-11, a novel anti-CD20 monoclonal antibody, for the detection of B cells. Oncol Lett 2020;20:1961–1967; doi: 10.3892/ol.2020.11753

33. Kato Y, Ohishi T, Yamada S, et al. Anti-CD133 monoclonal antibody CMab-43 exerts antitumor activity in a mouse xenograft model of colon cancer. Monoclon Antib Immunodiagn Immunother 2019;38:75–78; doi: 10.1089/mab.2019.0002

34. Kato Y, Furusawa Y, Yamada S, et al. Establishment of a monoclonal antibody PMab-225 against alpaca podoplanin for immunohistochemical analyses. Biochem Biophys Rep 2019;18:100633; doi: 10.1016/j.bbrep.2019.100633

35. Yamada S, Itai S, Nakamura T, et al. Detection of high CD44 expression in oral cancers using the novel monoclonal antibody, C(44)Mab-5. Biochem Biophys Rep 2018;14:64–68; doi: 10.1016/j.bbrep.2018.03.007

36. Yamada S, Itai S, Nakamura T, et al. Monoclonal antibody L(1)Mab-13 detected human PD-L1 in lung cancers. Monoclon Antib Immunodiagn Immunother 2018;37:110–115; doi: 10.1089/mab.2018.0004

37. Okada Y, Suzuki H, Kaneko MK, et al. Development of a sensitive anti-mouse CD39 monoclonal antibody (C39Mab-1) for flow cytometry and Western blot analyses. Monoclon Antib Immunodiagn Immunother 2024;43:24–31; doi: 10.1089/mab.2023.0016

38. Kaneko MK, Oki H, Ogasawara S, et al. Anti-podoplanin monoclonal antibody LpMab-7 detects metastatic lesions of osteosarcoma. Monoclon Antib Immunodiagn Immunother 2015;34:154–161; doi: 10.1089/mab.2014.0091

39. Kato Y, Kunita A, Abe S, et al. The chimeric antibody chLpMab-7 targeting human podoplanin suppresses pulmonary metastasis via ADCC and CDC rather than via its neutralizing activity. Oncotarget 2015;6:36003–36018; doi: 10.18632/oncotarget.5339

40. Oki H, Kaneko MK, Ogasawara S, et al. Characterization of monoclonal antibody LpMab-7 recognizing non-PLAG domain of podoplanin. Monoclon Antib Immunodiagn Immunother 2015;34:174–180; doi: 10.1089/mab.2014.0090

41. Asano T, Kaneko MK, Kato Y. Development of a novel epitope mapping system: RIEDL insertion for epitope mapping method. Monoclon Antib Immunodiagn Immunother 2021;40:162–167; doi: 10.1089/mab.2021.0023

42. Asano T, Kaneko MK, Kato Y. RIEDL tag: A novel pentapeptide tagging system for transmembrane protein purification. Biochem Biophys Rep 2020;23:100780; doi: 10.1016/j.bbrep.2020.100780

43. Asano T, Kaneko MK, Takei J, et al. Epitope mapping of the anti-CD44 monoclonal antibody (C(44)Mab-46) using the REMAP method. Monoclon Antib Immunodiagn Immunother 2021;40:156–161; doi: 10.1089/mab.2021.0012

44. Nanamiya R, Sano M, Asano T, et al. Epitope mapping of an anti-human epidermal growth factor receptor monoclonal antibody (EMab-51) using the RIEDL insertion for epitope mapping method. Monoclon Antib Immunodiagn Immunother 2021;40:149–155; doi: 10.1089/mab.2021.0010

45. Sano M, Kaneko MK, Aasano T, et al. Epitope mapping of an antihuman EGFR monoclonal antibody (EMab-134) using the REMAP method. Monoclon Antib Immunodiagn Immunother 2021;40:191–195; doi: 10.1089/mab.2021.0014

46. Sayama Y, Sano M, Kaneko MK, et al. Epitope analysis of an anti-whale podoplanin monoclonal antibody, PMab-237, using flow cytometry. Monoclon Antib Immunodiagn Immunother 2020;39:17–22; doi: 10.1089/mab.2019.0045

47. Tsuboyama K, Dauparas J, Chen J, et al. Mega-scale experimental analysis of protein folding stability in biology and design. Nature 2023;620:434–444; doi: 10.1038/s41586-023-06328-6

48. Fujii Y, Kaneko M, Neyazaki M, et al. PA tag: A versatile protein tagging system using a super high affinity antibody against a dodecapeptide derived from human podoplanin. Protein Expr Purif 2014;95:240–247; doi: 10.1016/j.pep.2014.01.009

49. Kato Y, Kaneko MK, Kuno A, et al. Inhibition of tumor cell-induced platelet aggregation using a novel anti-podoplanin antibody reacting with its platelet-aggregation-stimulating domain. Biochem Biophys Res Commun 2006;349:1301–1307; doi: 10.1016/j.bbrc.2006.08.171

50. Tamura R, Oi R, Akashi S, et al. Application of the NZ-1 Fab as a crystallization chaperone for PA tag-inserted target proteins. Protein Sci 2019;28:823–836; doi: 10.1002/pro.3580

51. Fujii Y, Matsunaga Y, Arimori T, et al. Tailored placement of a turn-forming PA tag into the structured domain of a protein to probe its conformational state. J Cell Sci 2016;129:1512–1522; doi: 10.1242/jcs.176685

52. Imaizumi Y, Takanuki K, Miyake T, et al. Mechanistic insights into intramembrane proteolysis by *E. coli* site-2 protease homolog RseP. Sci Adv 2022;8:eabp9011; doi: 10.1126/sciadv.abp9011

53. Tamura-Sakaguchi R, Aruga R, Hirose M, et al. Moving toward generalizable NZ-1 labeling for 3D structure determination with optimized epitope-tag insertion. Acta

Crystallogr D Struct Biol 2021;77:645–662; doi: 10.1107/S2059798321002527

54. Isoda Y, Tanaka T, Suzuki H, et al. Epitope mapping using the cell-based 2×alanine substitution method about the anti-mouse CXCR6 monoclonal antibody, Cx(6)Mab-1. Monoclon Antib Immunodiagn Immunother 2023;42:22–26; doi: 10.1089/mab.2022.0029

55. Isoda Y, Tanaka T, Suzuki H, et al. Epitope mapping of the novel anti-human CCR9 monoclonal antibody (C(9)Mab-11) by 2×alanine scanning. Monoclon Antib Immunodiagn Immunother 2023;42:73–76; doi: 10.1089/mab.2022.0035

56. Isoda Y, Tanaka T, Suzuki H, et al. Epitope mapping of an anti-mouse CXCR6 monoclonal antibody (Cx(6)Mab-1) using the 2×alanine scanning method. Monoclon Antib Immunodiagn Immunother 2022;41:275–278; doi: 10.1089/mab.2022.0019

57. Zebisch M, Krauss M, Schäfer P, et al. Crystallographic evidence for a domain motion in rat nucleoside triphosphate diphosphohydrolase (NTPDase) 1. J Mol Biol 2012;415:288–306; doi: 10.1016/j.jmb.2011.10.050

58. Schulte am Esch J, 2nd, Sévigny J, Kaczmarek E, et al. Structural elements and limited proteolysis of CD39 influence ATP diphosphohydrolase activity. Biochemistry 1999;38:2248–2258; doi: 10.1021/bi982426k

59. Spatola BN, Lerner AG, Wong C, et al. Fully human anti-CD39 antibody potently inhibits ATPase activity in cancer cells via uncompetitive allosteric mechanism. MAbs 2020;12:1838036; doi: 10.1080/19420862.2020.1838036

Address correspondence to:
Yukinari Kato
Department of Antibody Drug Development
Tohoku University Graduate School of Medicine
2-1, Seiryo-machi, Aoba-ku
Sendai, Miyagi 980-8575
Japan

E-mail: yukinari.kato.e6@tohoku.ac.jp